

Full Length Research Paper

Hybrid time-frequency domain adaptive filtering algorithm for electrodynamic shaker control

Martino O. A. Ajangnay

Electrical Engineering Department, College of Engineering and Architecture, University of Juba, South Sudan.
E-mail: Ajangnay16@hotmail.com.

Accepted 31 November, 2011

In this paper, adaptive filtering algorithm for control of the vibration force applied on the specimen in testing control systems is presented. Application for adaptive filtering especially in time domain is associated with a high computational complexity. This complexity is mitigated by using frequency-domain adaptive filtering scheme. In this paper, adaptive filtering algorithm in association with fast fourier transformation (FFT) was proposed. The algorithm was implemented using digital signal processor (DSP). The proposed algorithm show significant reduction in computational complexity as shown in results and discussion.

Key words: Hybrid frequency-time, adaptive filtering algorithm, electrodynamic shaker.

INTRODUCTION

Vibration design and control, aims either to eliminate or to reduce the undesirable vibration effects that may cause human discomfort and hazards, structural degradation and failure, performance deterioration and malfunction of machinery and processes. When a mechanical or electronic system is exposed to a vibration force, it causes the system to vibrate, producing an output response as a result of the vibratory excitation force. The control objective, in such a case, is to suppress the output response to a level that is acceptable. In an adaptive vibration control system, the vibration responses are explicitly sensed through transducers. This sensed response is fed to the controller producing the force that counteracts the effect of the vibration source, suppressing vibration at the sensing location. This force is applied to the system through the actuator. In this paper the electrodynamic shaker, with a permanent magnetic field, is used as a vibration exciter and the control algorithm adopted is a variant of adaptive control.

The application of adaptive control for shaker is motivated by the fact that some parameters of the shaker are time-varying (for example, coil inductance is frequency dependent, and the coil resistance may change with time as the result of skin effect and temperature). Also the specimen or load characteristic is usually unknown beforehand and it may be nonlinear. The shaker control algorithms proposed in the literature

(George, 1997; George and Dave, 2001), have been derived based on a linear shaker model or on the assumption that the load nonlinearity and variation of shaker parameters with time can be neglected. The performance of these controllers degraded when the shaker dynamics are time-varying or the load is highly nonlinear. Besides, the frequency domain adaptive filtering algorithm studied in IMV Corporation Japan, 2001 (Frain, 1977) suffers from high computational complexity and long time delay resulting from the utilization of the block frequency domain method. The limitations of these algorithms were addressed in this paper by utilizing a time and frequency block partitioning adaptive filtering algorithm to reduce the computational complexity, convergence time and the time delay. The electrodynamic shaker's main function is to deliver a force proportional to the current applied to its armature coil. These devices are used in such diverse activities as product evaluation, stress screening, squeak-and-rattle testing, and modal analysis.

The shakers may be driven by sinusoidal, random or transient signals, depending on the application. They are invariably driven by an audio-frequency power amplifier and may be used 'open loop' (as in most modal testing) or under closed-loop control, where the input to the driving amplifier is servo-controlled to achieve a desired motion level in the device under test. There are three

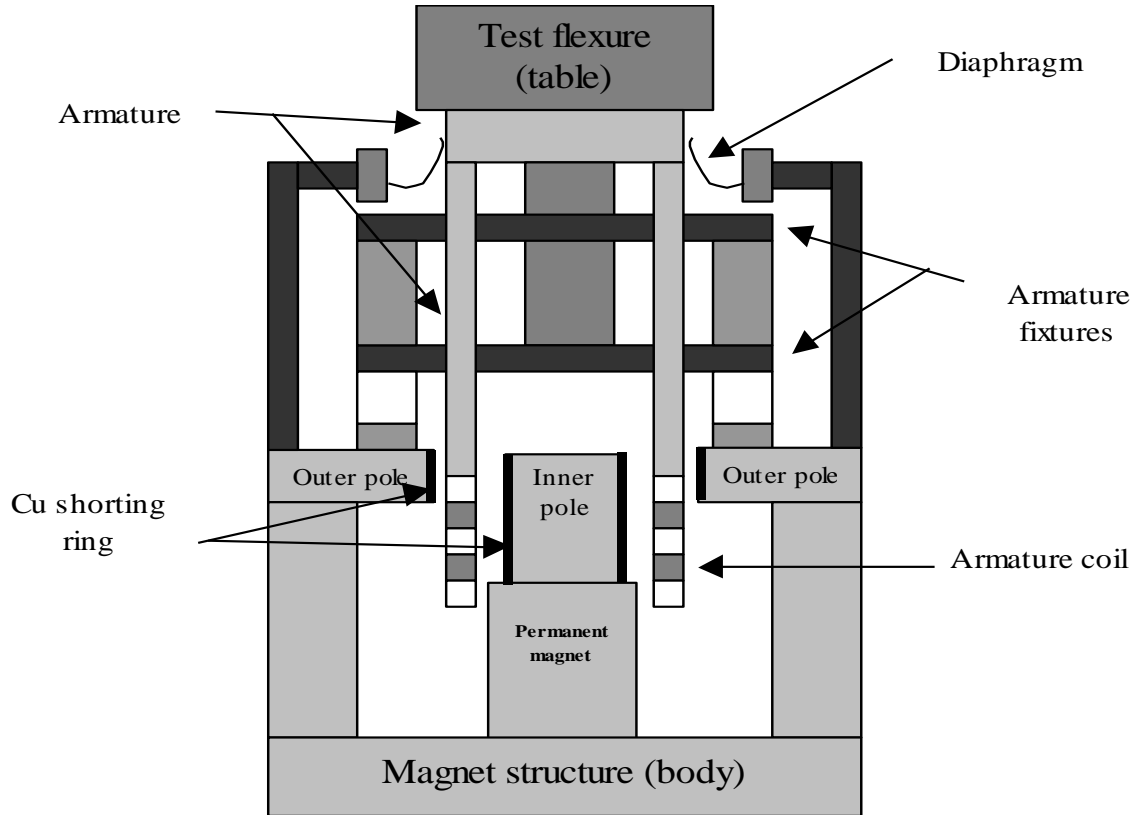


Figure 1. Electrodynamic shaker cross-section.

major shaker types widely used (Hydraulic, Inertial and Electrodynamic Shakers) in vibration testing. However, electrodynamic shakers have many advantages compared to the other types due to their high output bandwidth and moderate input power requirements. In the vibration control system with the shaker used as an exciter, it is essential to characterize the shaker dynamic model and to compute the shaker mechanical and electrical parameters that will be used in the simulation stage. An initial experiment is performed by monitoring the voltage input to the power amplifier or the current delivered by the power amplifier, and measuring the dynamic response of the shaker (accelerometer signal) with a bare shaker table, then with a known table load (George, 1997; De Silva, 2000).

The schematic depicted in Figure 1 shows a sectioned view of a permanent magnet electrodynamic shaker with emphasis on the magnetic circuit and the suspended driving table. At the heart of the shaker is a single-layer armature coil of copper wire, suspended in a uniform radial magnetic field. When a current is passed through the coil, a longitudinal force F is produced in proportion to; the current I flowing in the coil, the length l of the coil in the magnetic field, and the strength B of the field flux. This force is transmitted to the table structure to which the device under test is attached. The generated force in

the armature coil is mathematically expressed as (Frain, 1977).

$$F = BIl \tag{1}$$

Where, F , is the armature coil force, (N); B , is the magnetic flux density, (T); l , is the length of armature coil in the field, (m); I , is the armature coil current, (A).

SYSTEM MODELLING OF ELECTRODYNAMIC SHAKER

The electrodynamic shaker can be expressed as a current driven or voltage, transfer function. In the current driven transfer function mode, the acceleration frequency response is plotted as current supplied by the power amplifier against the shaker acceleration response. In this case, the effect of electromagnetic damping is not evidenced. The frequency response plot reflects only the structural damping terms, those that could be measured with external excitation applied to the shaker with its drive coil un-terminated. The same low damping factors are usually evident when a current amplifier drives the shaker. In contrast, the voltage driven transfer function (voltage applied to the shaker system against the acceleration, reflects the significant electromagnetic damping applied

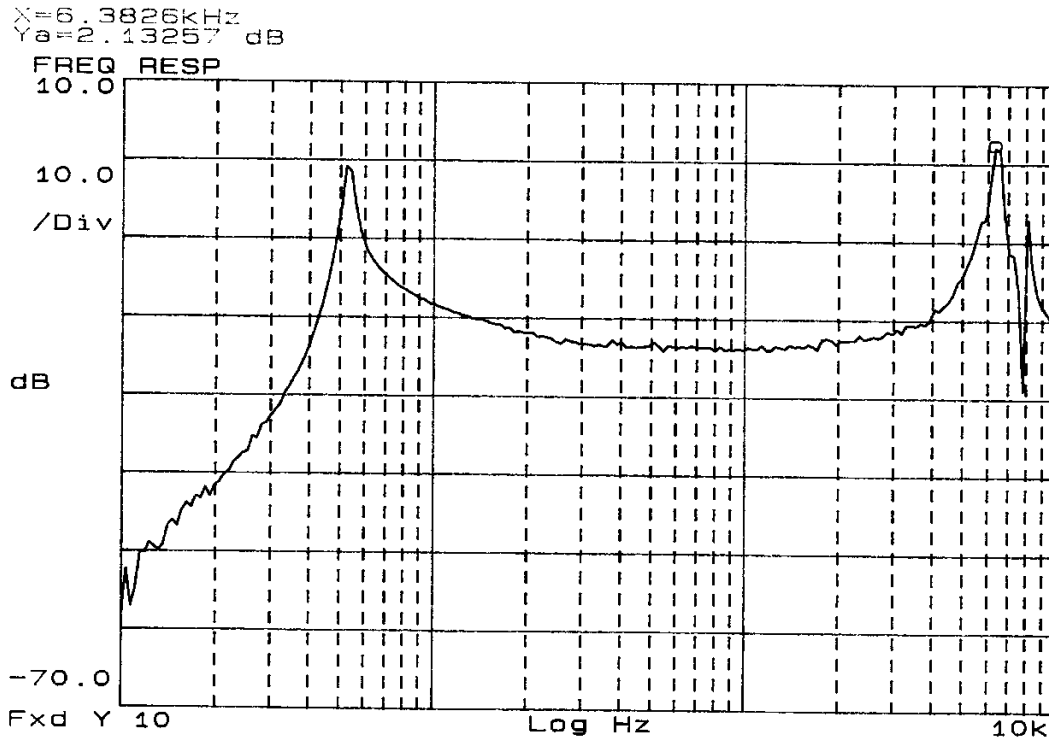


Figure 2. Current driven transfer function of the unloaded electrodynamic shaker.

by the cross-coupling terms between the electrical and mechanical components of the system (George, 1997; Haykin, 2002). The force provided by the shaker is given by $F = BIl$. Figures 2 and 3 show, respectively, the current-driven and voltage-driven frequency response when the swept sine signal of amplitude 0.7 v was applied to shaker power amplifier. The shaker mechanical model is modelled by assuming the armature structure is elastic rather than rigid.

This gives the shaker mechanical model three degrees-of-freedom. This is achieved by modelling the coil and table as separate masses connected by springs and dampers (George, 1997; George and Dave, 2001). In order to compute the mechanical and electrical parameters of the electrodynamic shaker and the associated load, a swept sine test is conducted to compute the frequency response function as the ratio between the shaker’s output response (accelerometer signal), and the input supply voltage (voltage mode). The resonance frequencies in the operating range and the half-power points are recorded. These are used in mathematical formulas (Equation 1), to estimate the masses, damping constant, spring stiffness, and electrical impedance. Some of the parameters are tuned using trail and error during simulation, so that the simulated frequency response matches the measured frequency response shape. The mathematical equations used to deduce the mechanical and electrical parameters

from the frequency response, are given by IMV Corporation Japan (2001).

$$\begin{aligned}
 M_e &= \frac{M_a f_a}{f_n^2 - f_a^2} \\
 K &= (2\pi f_n)^2 M_e \\
 D &= 2\pi \Delta f_{3dB} M_e
 \end{aligned}
 \tag{2}$$

Where;

- M_e effective mass of the shaker system
- M_a mass of the load
- K spring stiffness
- D damping factor
- f_n resonance frequency when the shaker has no load (6.38 kHz)
- f_a resonance frequency when the shaker is loaded
- Δf_{3dB} half - power (-3dB) points bounding resonance frequency f_n

Electrical equivalent model

The electrical model of the electrodynamic shaker consists of the coil resistance R and inductance L . The electrical impedance of the shaker coil reflects the

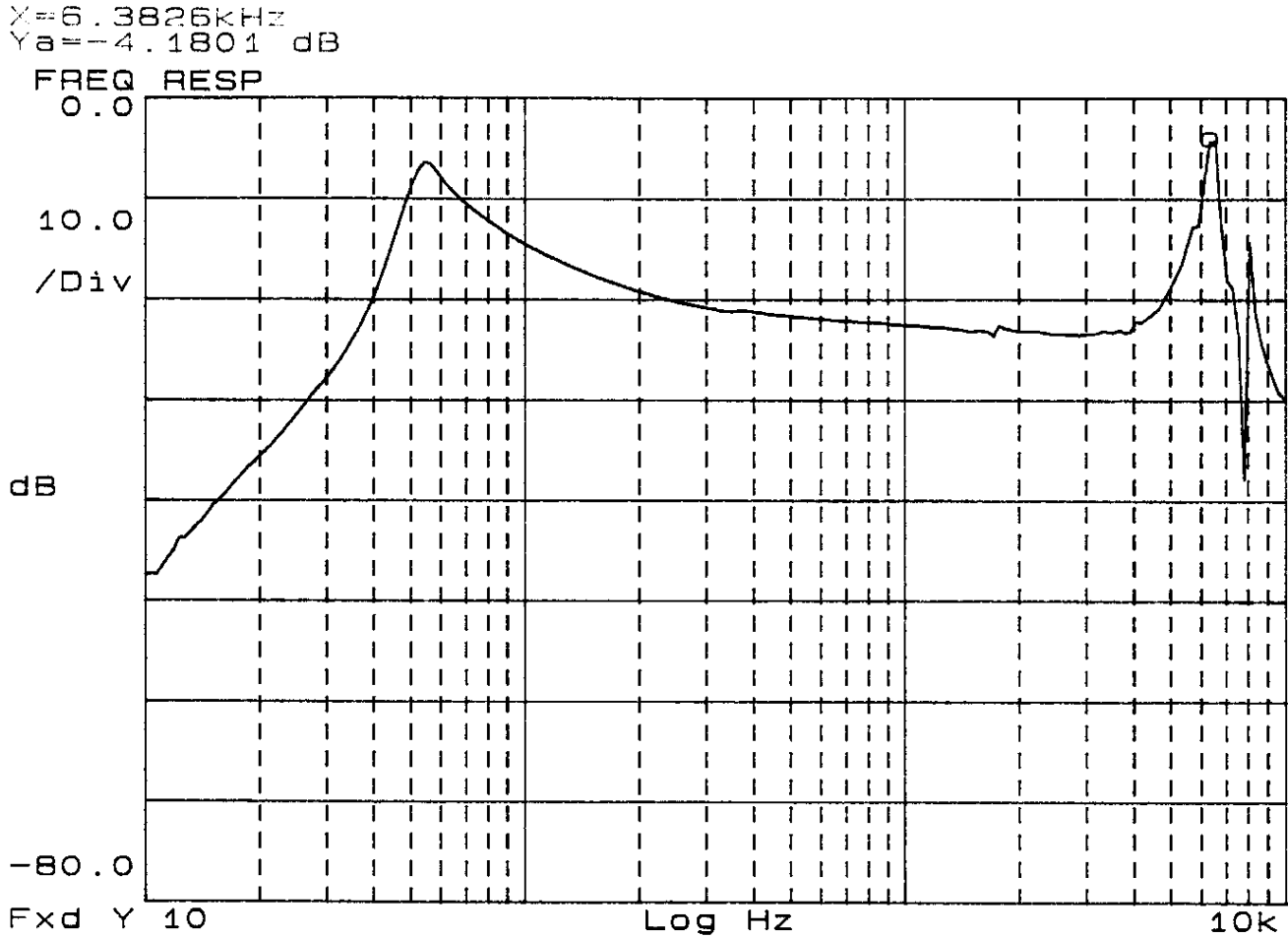


Figure 3. Voltage driven transfer functions of the unloaded electrodynamic shaker.

mechanical motion of the shaker table. When the coil moves in the magnetic field, a voltage is generated across the coil proportional to the motion velocity ($E = Bl$ $u = \alpha u$). Thus the voltage at the coil terminals may be written in terms of the flowing current i and the velocity u as:

$$v = Ri + L \frac{di}{dt} + \alpha u \tag{3}$$

Where $\alpha = Bl$ is constant, called the transduction factor. The mechanical mobility (velocity/force) of the shaker mechanical components may be represented by a driving-point frequency response function H_{fu} , so that

$$u = H_{fu} F \tag{4}$$

The coil produces an axial force, acting on the shaker mechanical elements, in proportion to the applied current.

$$F = \alpha i \tag{5a}$$

Combining equations (3, 4 and 5), yields the impedance Z exhibited by the coil.

$$Z = \frac{v}{i} = R + j2\pi fL + \alpha^2 H_{fu} \tag{5b}$$

The minimum coil impedance is determined by the differential (dc) resistance, which is real-valued. The coil inductance contributes an imaginary (90° phase-shifted) ac component that increases in direct proportion to frequency. The mechanical mobility contributes frequency-dependent terms that exhibit a real maximum at each mechanical resonance. These can significantly increase the impedance in a narrow frequency band. The effective resistance and inductance of the coil can be measured by clamping the fixture table (locked rotor test). The equivalent circuit is shown in Figure 4 where R_1 and L_1 are the resistance and leakage inductance of the moving coil, R_2 and L_2 are the resistance and leakage inductance of the copper pole-plating, and L_m is the moving coil magnetizing inductance. Using current mesh

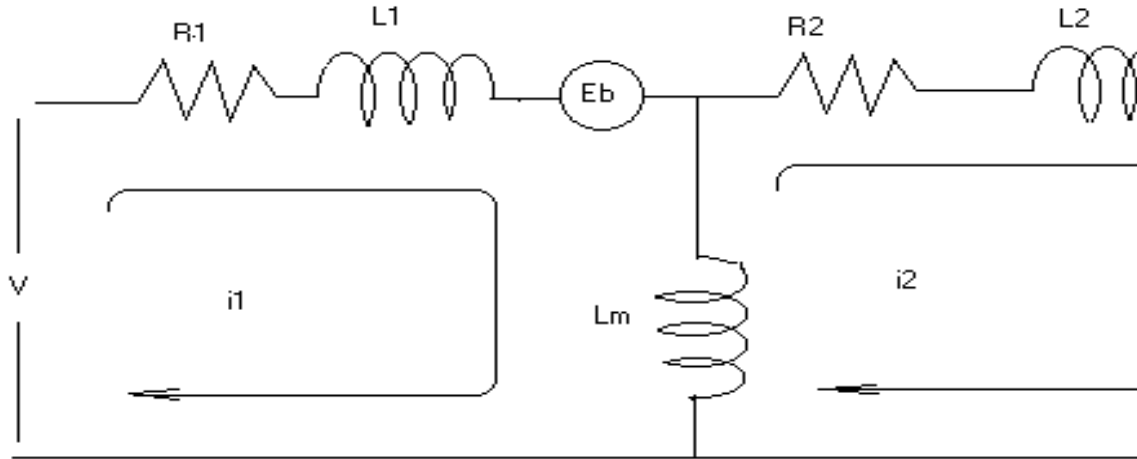


Figure 4. Moving coil T-circuit showing the short-circuit secondary.

analysis, the mathematical equations for the shaker electrical model can be derived from Figure 3 as

$$v = R_1 i_1 + L_1 \frac{di_1}{dt} + L_m \left(\frac{di_1}{dt} - \frac{di_2}{dt} \right) + \alpha \frac{dl_1}{dt} \quad (6)$$

$$0 = R_2 i_2 + L_2 \frac{di_2}{dt} + L_m \left(\frac{di_2}{dt} - \frac{di_1}{dt} \right)$$

$$\alpha i_1 = M_1 \frac{d^2 l_1}{dt^2} + K_1 (l_1 - l_2) + D_1 \left(\frac{dl_1}{dt} - \frac{dl_2}{dt} \right)$$

$$K_1 (l_1 - l_2) + D_1 \left(\frac{dl_1}{dt} - \frac{dl_2}{dt} \right) = M_2 \frac{d^2 l_2}{dt^2} + K_2 (l_2 - l_3) + D_2 \left(\frac{dl_2}{dt} - \frac{dl_3}{dt} \right) \quad (7)$$

$$K_2 (l_2 - l_3) + D_2 \left(\frac{dl_2}{dt} - \frac{dl_3}{dt} \right) = M_3 \frac{d^2 l_3}{dt^2} + K_3 l_3 + D_3 \frac{dl_3}{dt}$$

Mechanical equivalent model

The shaker mechanical system includes a means for storing potential energy (spring), a means for storing kinetic energy (mass or inertia), and a means by which energy is gradually lost (dampers). The mechanical model of the shaker consists of two distinct elements, the moving coil and the fixture table. The fixture table is suspended by a suspension flexure to the shaker body assembly. The fixture table can be modelled as a pair of masses M_2 and M_3 , with flexure stiffness, K_2 and K_3 , and damping coefficients, D_2 and D_3 . The moving coil of mass M_1 is adhered to the fixture table by an adhesive bonding, which also can be characterized by a spring with a finite stiffness K_1 and a damping element with coefficient D_1 . Thus Figures 4 and 5 can represent the unloaded shaker electrical and mechanical systems, respectively. The mechanical system and mathematical equations can be expressed as:

$$\alpha i_1 = M_1 \frac{d^2 l_1}{dt^2} + K_1 (l_1 - l_2) + D_1 \left(\frac{dl_1}{dt} - \frac{dl_2}{dt} \right)$$

$$K_1 (l_1 - l_2) + D_1 \left(\frac{dl_1}{dt} - \frac{dl_2}{dt} \right) = M_2 \frac{d^2 l_2}{dt^2} + K_2 (l_2 - l_3) + D_2 \left(\frac{dl_2}{dt} - \frac{dl_3}{dt} \right) \quad (7)$$

$$K_2 (l_2 - l_3) + D_2 \left(\frac{dl_2}{dt} - \frac{dl_3}{dt} \right) = M_3 \frac{d^2 l_3}{dt^2} + K_3 l_3 + D_3 \frac{dl_3}{dt}$$

PARTIALLY HYBRID TIME-FREQUENCY DOMAIN ADAPTIVE FILTERING ALGORITHM

In vibration testing control systems, the shock test is conducted to simulate the effect of the shock that a specimen is expected to be subjected to, during its lifetime. To prevent testing damage, it is essential that the test be controlled such that the shaker output converges smoothly to the intended reference shock pulse. Usually, in shaker vibration control, the load dynamics are not well defined before hand. Thus, the control algorithm must be designed with the following consideration:

- (1) The controller should be able to update its parameters to cope with load uncertainty.
- (2) The controller must have a fast response, especially when the pulse used is a shock pulse; and
- (3) The controller must be robust, such that it can adapt to a large range of load variations.

The following give a brief description of inverse adaptive filtering, time domain adaptive filtered-x filtering and hybrid time-frequency domain adaptive filtering algorithms.

Inverse adaptive filtering algorithm

For tracking control or servo-control systems, the inverse

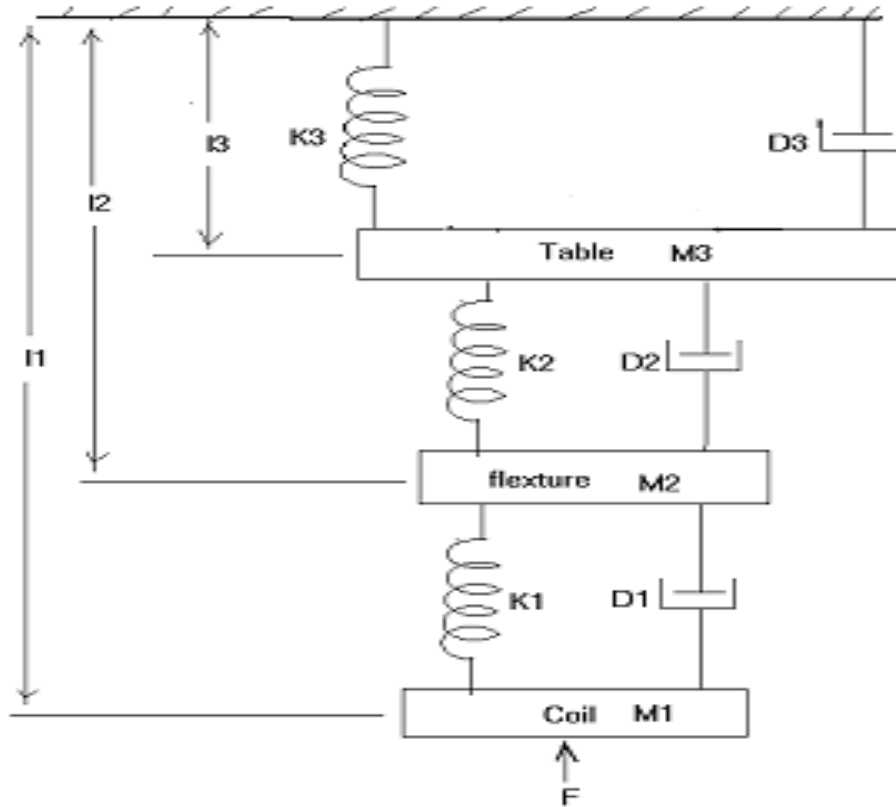


Figure 5. Mechanical equivalent circuit of the unloaded electrodynamic shaker.

of the system dynamics can be employed as a controller such that, when the inverse model is cascaded with the system dynamics, the overall system output converges to the reference input. This configuration of the inverse model and system dynamics constitutes a feed-forward control system. Adaptive feed forward techniques have been used widely in the active control of sound and vibration (Olmos et al., 2002; Valoor et al., 2000). The application of the shaker inverse model as a controller has been reported in Macdonald (1994), where the shaker and controller were modelled in the frequency domain. Cascading the adaptive filter with the unknown system causes the adaptive filter to converge to a solution that is the inverse of the unknown system. Therefore, inverse modelling is motivated by the fact that, when the transfer function of the unknown system is $W(z)$ and the adaptive filter transfer function is $C(z)$, then error measured between the desired signal and the signal from the cascaded system reaches its minimum when the product of $W(z)$ and $C(z)$ is 1.

$$W(z)C(z) = 1 \quad (8)$$

For the previous relation to be true, $W(z)$ must be equal $[C(z)]^{-1}$, the inverse of the transfer function of the unknown system. In practice, it is sometimes essential to

have prior knowledge of the system dynamics, so that an accurate inverse of the dynamic system can be obtained. For example, if the system under investigation is known to be minimum-phase, that is, has all of its zeros inside the unit circle in the z-plane, then the inverse will be stable with all its poles inside the unit circle. When the plant is non-minimum-phase, then some of the poles of the inverse will be outside the unit circle and the inverse will be unstable. It is also essential to consider the effect of transport delay in the system. For instance, when the unknown system is cascaded with the filter, the output signal from the cascaded system reaches the summation points after it has been delayed by a time equal to the unknown system delay plus the filter delay.

To prevent the adaptive filter from trying to adapt to a signal it has not yet seen (equivalent to predicting the future), the desired signal is delayed, with the number of samples equivalent to half the length of the adaptive filter. Figure 6 shows the block diagram for modelling the inverse of the electrodynamic shaker using a finite impulse response (FIR) filter. Assuming the shaker and the payload are linear, then the commutation rule applies, such that the controller and plant position can be interchanged. Assuming the input signal $r(n)$ is applied to the shaker and a payload, the acceleration response Output $a(n)$ will act as the input to the FIR filter. The

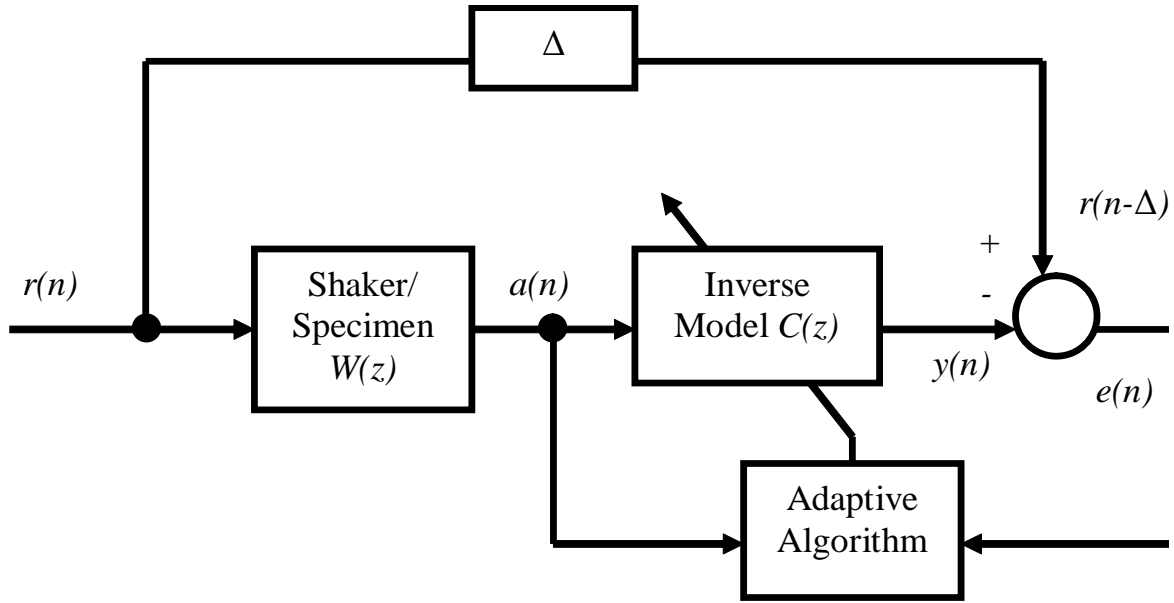


Figure 6. Inverse adaptive modelling block diagram.

output response of the cascaded system is given by

$$y(n) = \sum_{i=0}^{L-1} c_i(n)a(n-i) \quad (9)$$

Where L is the number of weights in the FIR filter and $c_i(n)$ is the i^{th} weight of the adaptive filter at iteration n . The error between the delayed input signal and the output of the cascaded system is

$$e(n) = r(n - \Delta) - y(n) \quad (10)$$

Where Δ is the sample delay, equal to $L/2$. Using the Least mean squares (LMS) algorithm, the weights of the inverse adaptive filter are updated using the following formula

$$c(n+1) = c(n) + \mu e(n)a(n) \quad (11)$$

Where μ is the step-size, and the weight vector $c(n)$ and filter regression input vector $a(n)$ are given by equations (5a) and (5b), respectively.

$$c(n) = [c_0(n), c_1(n), \dots, c_{L-1}(n)]^T \quad (12)$$

$$a(n) = [a(n), a(n-1), \dots, a(n-L+1)]^T \quad (13)$$

Filtered-x adaptive filtering algorithm

The filtered-x algorithm has been extensively applied in

the active control of sound and vibration. The design is carried out in two phases. In the first phase, the model of the dynamic system to be controlled is computed. In the second phase, the controller weights are updated, and the optimal values found are implemented to control the dynamic system. The main feature of the filtered-x algorithm is that the signal used in the controller weights adaptation, is produced by filtering the reference input signal, via the system model weights. Figure 7 illustrates the block diagram of the filtered-x adaptive filtering algorithm for the electrodynamic shaker. Assume the model of the shaker and the specimen has been computed. Let the number of weights in the shaker/specimen model and the control filter be L_c and L_p , respectively. The output response of the FIR filter controller is computed as a convolution of the FIR filter weights and the input reference signal.

$$u(n) = \sum_{i=0}^{L_c-1} c_i(n)r(n-i) \quad (14)$$

The FIR filter output is applied to the shaker/specimen, generating the acceleration output of $a(n)$. The error signal is computed as the difference between the delayed input signal and the shaker/specimen acceleration output response.

$$e(n) = r(n - \Delta) - a(n) \quad (15)$$

Where Δ is the time delay. The input reference signal is filtered through the shaker model weights to generate the

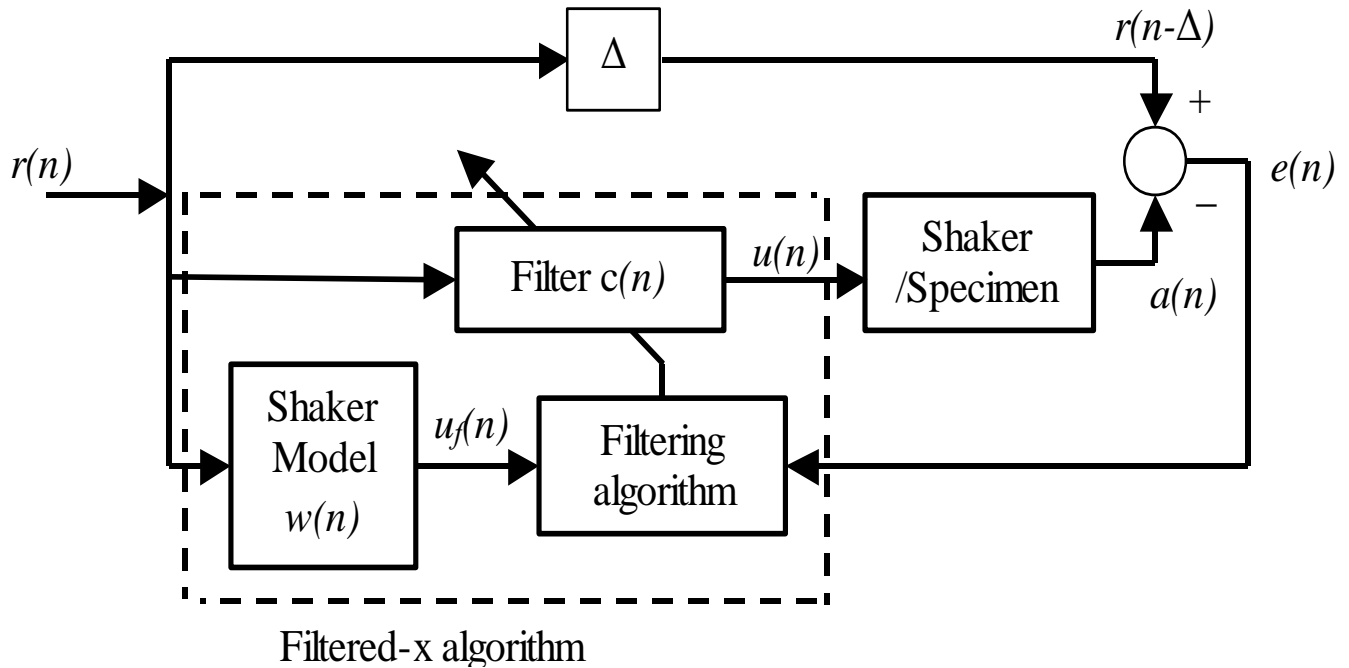


Figure 7. Filtered-x adaptive filtering block diagram.

filtered signal $u_f(n)$ given by

$$u_f(n) = \sum_{i=0}^{L_p-1} w_i(n)r(n-i) \tag{16}$$

Using the LMS algorithm, the controller weights are updated using

$$c(n+1) = c(n) + \mu e(n)u_f(n) \tag{17}$$

Where μ is the step-size, $c(n)$ is the controller weight vector, and $u_f(n)$ is the regression vector. The controller weight vector is given by

$$c(n) = [c_0, c_1, \dots, c_{L_c-1}]^T \tag{18}$$

The regression vector is defined as

$$u_f(n) = [u_f(n), u_f(n-1), \dots, u_f(n-L_p+1)]^T \tag{19}$$

Partially hybrid time-frequency domain adaptive filtering (PHTFDAF) algorithm

Here, partially hybrid time-frequency domain adaptive filtering (PHTFDAF) algorithms are described for modelling and controller design for the shock control of the electrodynamic shaker. The model and inverse model

of the electrodynamic shaker are modelled by an FIR filter. Experimental results show that the model and inverse model of the shaker required thousands of FIR weights to represent the dynamic system (shaker and load attached) effectively. This large number of filter taps results in complex computation and implementation and in real-time requires large resources, in terms of memory. As a result, it is impractical to use time-domain filtering methods to find the model and inverse model of the electrodynamic shaker and its load. Computational complexity and convergence speed of the FIR model's weights to their optimal values was addressed using the frequency domain adaptive filtering algorithm studied in partially hybrid time-frequency domain adaptive filtering (PHTFDAF) algorithm. However, the conventional frequency domain adaptive filtering algorithm has a drawback of inherent delay between the block input and the system output response, especially during the initial stages while the input block data collection is processing.

The problem of the long delay in frequency domain adaptive filtering was addressed by splitting the time domain filter weights sequentially into non-overlapping partitions (Olmos et al., 2002; Valoor et al., 2000). Although partitioning of the filter weights results in a small input block size, it does not completely eliminate the system time delay. A delay less frequency domain adaptive filtering algorithm was proposed in Bendel et al. (2001), where the system delay is eliminated by adapting the first partition weights using a time domain algorithm and adapting the remaining partitions using a frequency domain adaptive filtering algorithm. Although this method

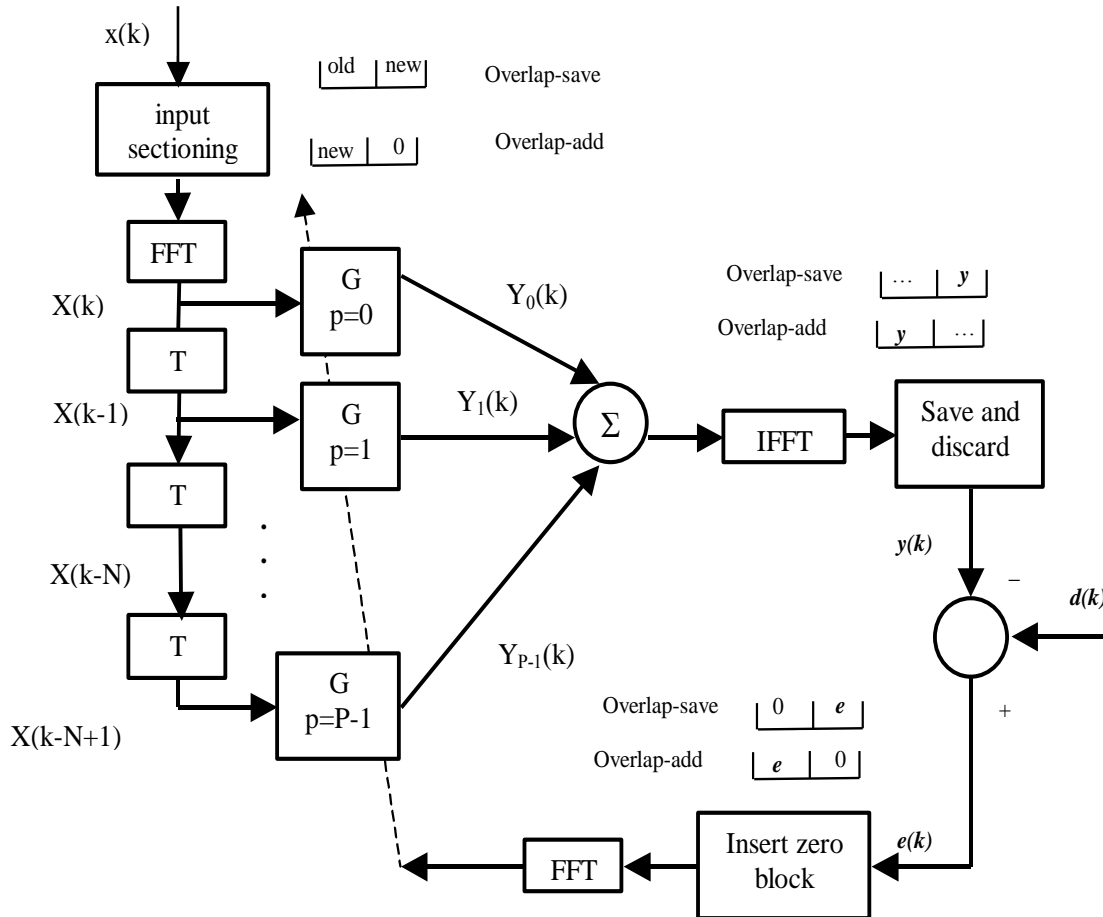


Figure 8. Partitioned frequency domain adaptive filtering block diagram.

eliminates the time delay in adaptation, it increases computational complexity due to the use of the time domain adaptive filtering method in updating the first partition weights. To reduce the computational complexity of partitioned frequency domain adaptive filtering, the PHTFDAF algorithm was proposed. In the PHTFDAF algorithm, the time domain filter weights are sequentially divided into non-overlapping partitions. The first partition weights are adapted using the time domain only during the initial stage. Then these weights are adapted using the frequency domain algorithm as well as the other partition's weights.

This method of partially updating some weights in the time domain and then in the frequency domain reduces the computational complexity of the whole adaptation process, as well as minimising the time delay in the adaptation process. The proposed algorithm for adaptive control is different from the one reported in Olmos et al. (2002), and Bendel et al. (2001). The time domain adaptive filtering of the model and its inverse are sequentially split into non-overlapping partitions and the first partition weights are updated only in the time domain during the first block input data collection, then they are

adapted in the frequency domain in the remaining adaptation periods along with the other partitions weights.

PBFDAF algorithm

The computational complexity and long time-delay problems, associated with the conventional frequency domain adaptive filtering algorithm, can be minimized by using the partitioned block frequency domain adaptive method, in which the weights of the FIR filter are sequentially split into non-overlapping partitions. Then the frequency domain adaptive algorithm is applied to each partition. The main advantage of PBFDAF over the non-partitioned algorithm is that a small processing block size is required; consequently, the delay of the PBFDAF is small. Figure 8 shows the PBFDAF block diagram. To derive the equations that govern the PBFDAF algorithm, assume that the FIR filter has M weights, divided into P partitions, each partition containing N weights. Therefore the output of the blocks of N samples is given by

$$y_k = [y(kN), \dots, y(kN + N - 1)]^T = \sum_{p=0}^{P-1} A(k-p) [w_{pN}(kN), \dots, w_{(p+1)N-1}(kN)]^T \quad (20)$$

Where $A(k)$ is an $N \times N$ matrix whose i, j element is given by

$$A_{i,j}(k) = x(kN + i - j), \quad i, j = 0, 1, \dots, N - 1$$

The output of each partition is a circular convolution of the partition input with the weight vector of the partition at the k^{th} time, where for example, the input of the partition (overlap-save) and weight vector per partition are, respectively.

$$\begin{aligned} \mathbf{x}(k-p) &= [x([k-p-1]N), \dots, x([k-p]N), \dots, x([k-p+1]N-1)]^T \\ \mathbf{w}_p(k) &= [w_p(kN), \dots, w_{(p+1)N-1}(kN), 0, \dots, 0]^T \end{aligned} \quad (21)$$

Thus the input and partition weight vector in the frequency domain are defined as

$$\begin{aligned} \mathbf{X}(k-p) &= \text{diag}(F\mathbf{x}(k-p)), \quad p = 0, 1, \dots, P-1 \\ \mathbf{W}(k) &= F\mathbf{w}_p(k) \quad p = 0, 1, \dots, P-1 \end{aligned} \quad (22)$$

Where F denotes the discrete Fourier transform (DFT) operator of order $2N$. For the overlap-save method of the block sectioning, the adaptive filter output in the time domain is

$$y_k = [y(kN), \dots, y(kN + N - 1)]^T = [0_n \ I_n] F^{-1} \sum_{p=0}^{P-1} Y_p(k) \quad (23)$$

$$\text{where } Y_p(k) = \mathbf{X}(k-p)\mathbf{W}_p(k)$$

where $[0_n \ I_n]$ is $N \times 2N$, is the output projection matrix used to force the first element of the output vector to zero as a result of the application of the overlap-save sectioning on the input block. The weight update of each partition is defined as

$$\mathbf{W}_p(k+1) = \mathbf{W}_p(k) + 2\mu F \left(\begin{bmatrix} I_N & 0_N \\ 0_N & 0_N \end{bmatrix} F^{-1} \{ \mathbf{X}^*(k-p)\mathbf{E}(k) \} \right) \quad (24)$$

Where $\mathbf{E}(k)$ is the error vector in the frequency domain and is defined as

$$\mathbf{E}(k) = F(\mathbf{e}(k)) = F[0, 0, \dots, 0, e(kN), \dots, e(kN + N - 1)]^T \quad (25)$$

EXPERIMENTAL SETUP

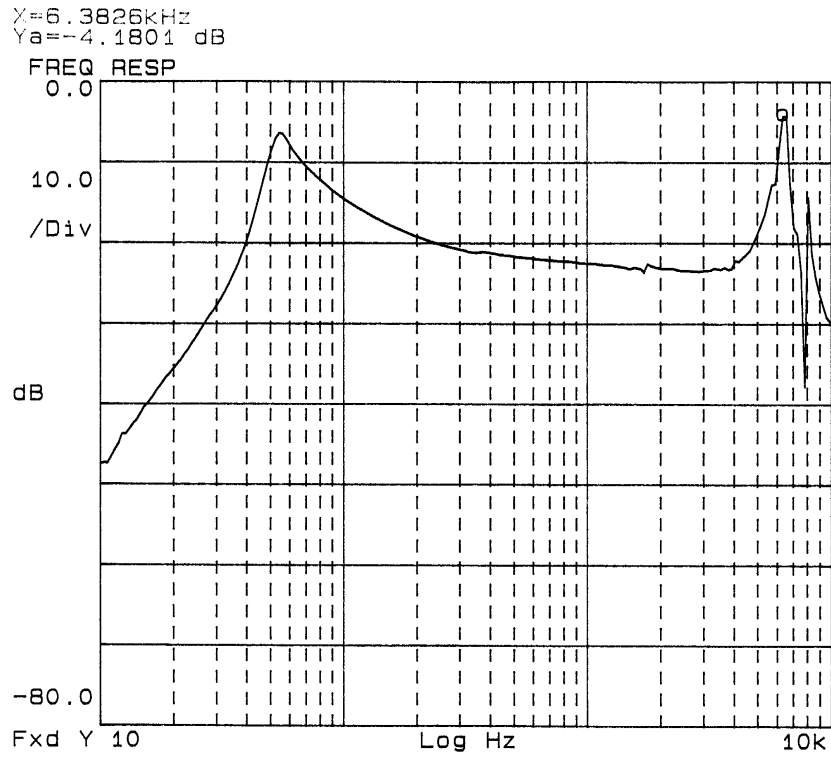
In this paper, the loaded shaker was characterized using a swept sine signal, generated from the HP 3562A Dynamic Signal Analyzer Figure 15. The signal, swept from 10 Hz to 10 kHz, was applied to the shaker/specimen via the power amplifier. The acceleration output response was measured via a charge amplifier, whose output was connected to the 2nd channel of the Dynamic Signal

Analyzer. The frequency response was computed as the ratio between output acceleration measured by charge amplifier and the input swept sine signal of 0.7 v rms amplitude. The charge amplifier sensitivity and scale values were set to 80 pC/g and 5 g/V, respectively. From the measured transfer function of the unloaded shaker (Figure 9a), the upper resonance frequency occurs at 6.38 kHz and low resonance at 54.32 Hz. The resonance frequency values from Figure 9a and the half-power values were used to compute masses, and springs and damper constants of the mechanical system. Some electrical components were measured. The remaining electrical and mechanical parameters were approximated using trail-and-error, by tuning the simulation program till the frequency response matched the measured frequency response. The frequency response of the unloaded shaker model is shown in Figure 9b.

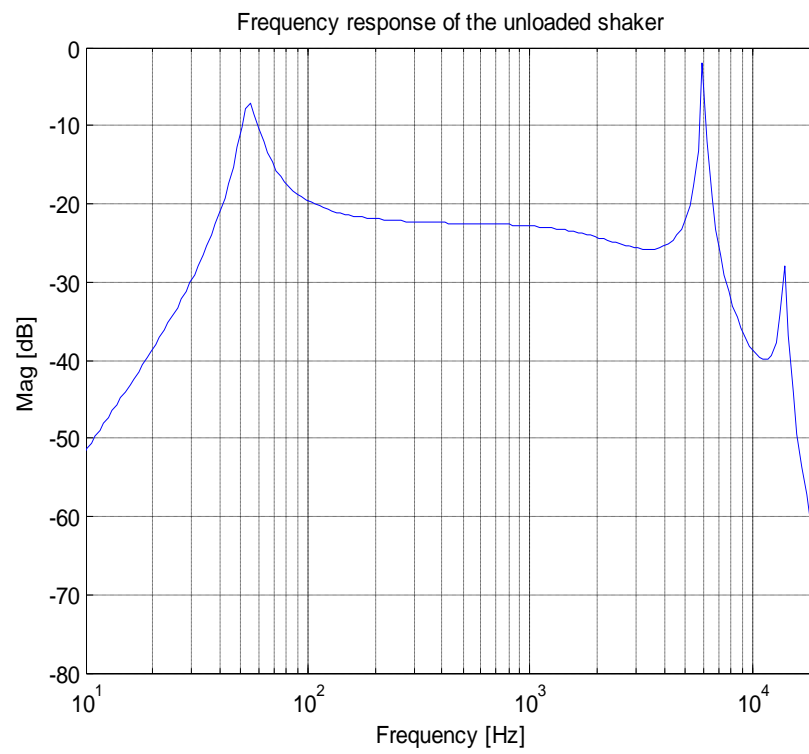
RESULTS AND DISCUSSION

The shaker model represented by the FIR adaptive filter is identified using the partially hybrid frequency domain adaptive filtering algorithm described in partially hybrid time-frequency domain adaptive filtering algorithm. The FIR filter representing the model has 1024 weights. The time-domain weights are divided into two partitions, each of 512 taps, as is explained in the previous sections. The weights of the first partition are adapted using the non-block time domain filtering algorithm only in the first block input stage ($n = 0, 1, \dots, 511$). In subsequent block input iterations, the weights in the first partition and the weights of the other partitions are updated using the frequency domain adaptive filtering algorithm. After the shaker model is computed, the model weights are used in the PHTFDAF FIR controller model, such that when the resultant FIR controller is connected in cascade with the shaker, the shaker output tracks the reference input signal. That is, the control objective can be stated as: given the desired input reference signal and the shaker model, it is required to compute the FIR controller model such that when cascaded with the shaker, the output of the shaker tracks the reference input signal (Figure 10).

The transition of the shaker controlled output response to the input reference signal should occur in a short time (due to the shock pulse width, usually 2 to 20 ms) and converge smoothly (no overshoot). The control model is represented by an FIR filter of 1024 weights. The weights are divided into two partitions, each of 512 weights, as in the case of the system identification of the shaker model. Using the filtered-x method in the time and frequency domains, the shaker output tracks the reference signal. The adaptation process converges to the optimal values after 20 block input iterations. The input reference signal and shaker controlled output responses are shown in Figures 11 and 12, respectively. From comparison of the desired input reference signal (Figure 11) and the shaker-controlled output (Figure 12), it is seen that the shaker output tracks the input reference signal. The control algorithm implementation results in a reduction in the ringing of the shaker output response. The rise time and



(a)



(b)

Figure 9. Frequency response of the unloaded shaker: (a) practical and (b) simulation.

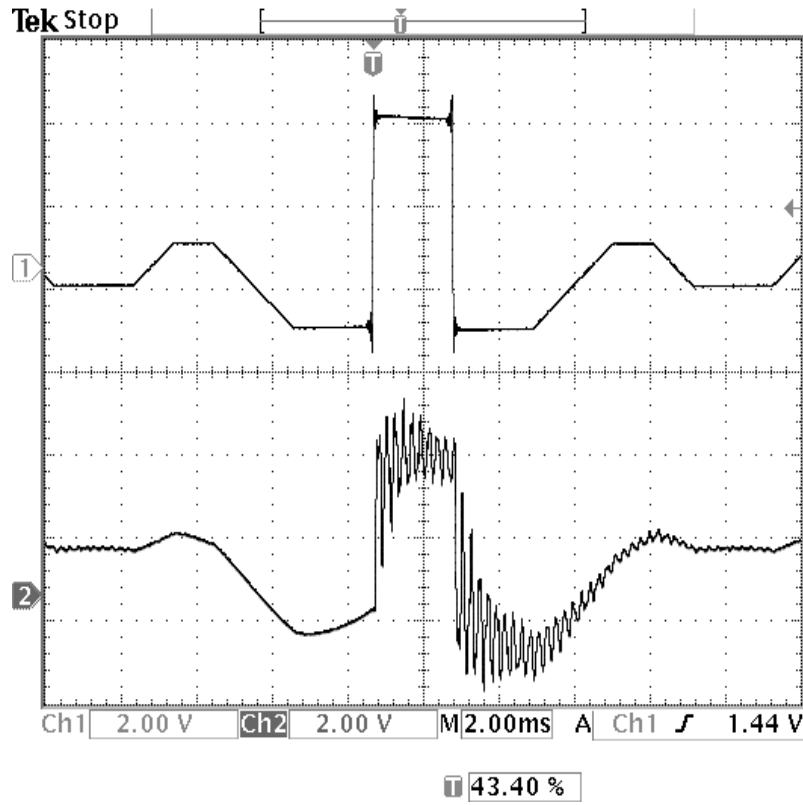


Figure 10. Shaker input reference and shaker output response.

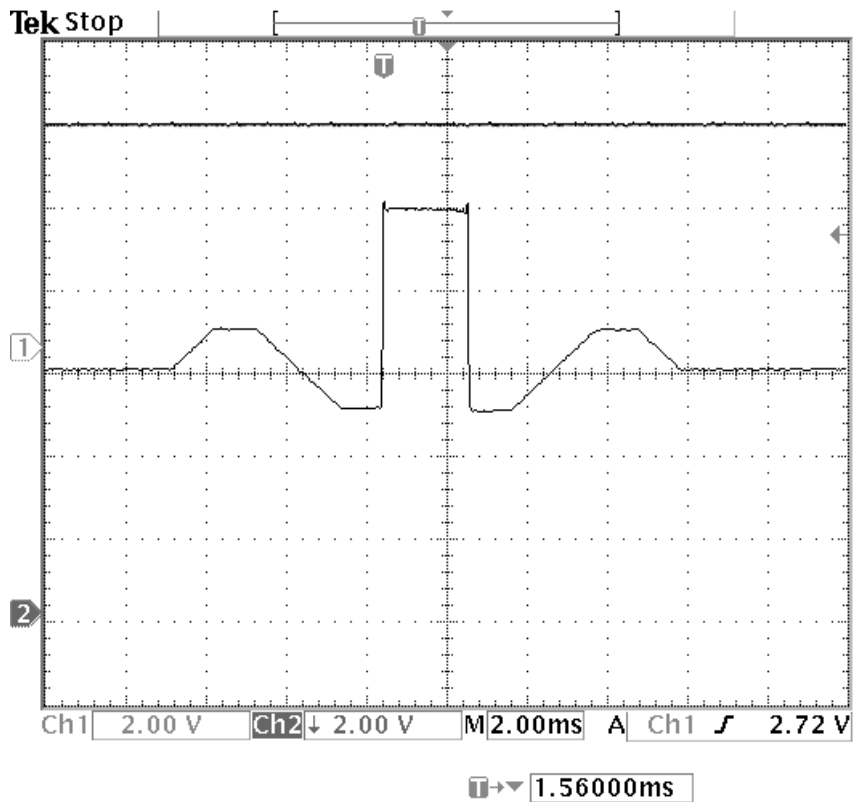
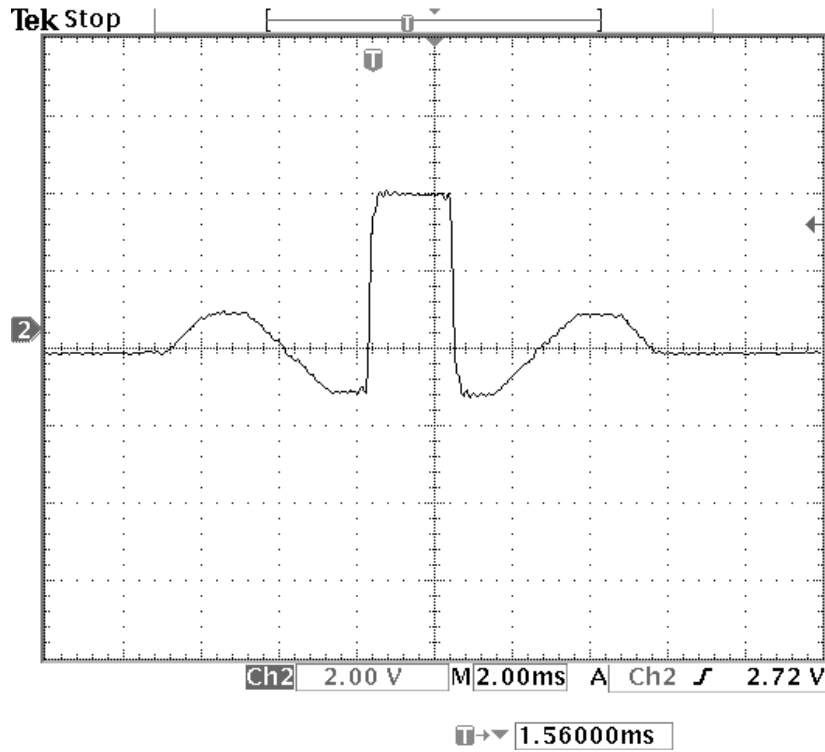
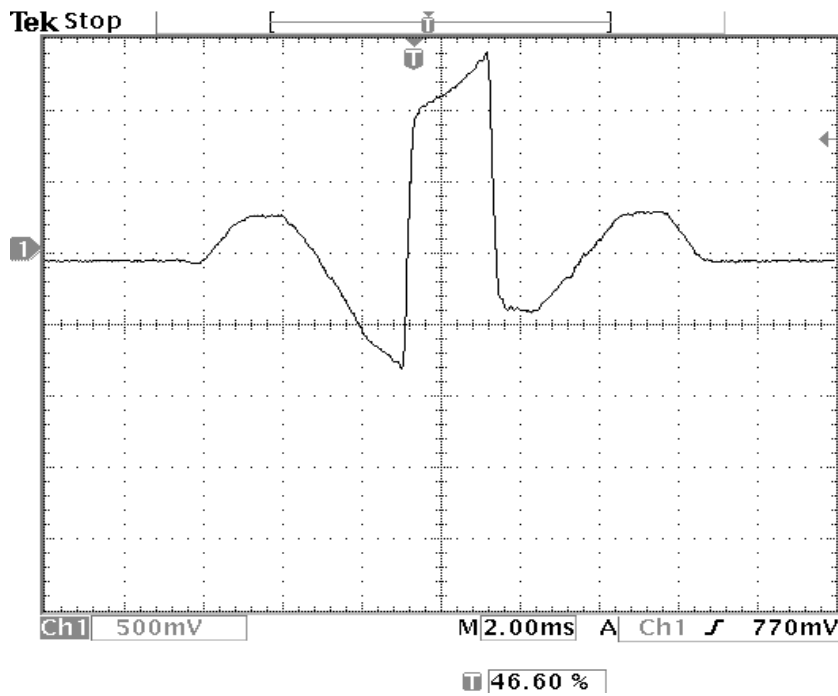


Figure 11. Input reference.



12 Feb 2004
13:10:15

Figure 12. Shaker controlled output (with PHTFDAF).



12 Feb 2004
13:36:02

Figure 13. Controller output (Shaker input- (with PHTFDAF).

settling time achieved are 0.05 and 0.85 ms, respectively. The controller output signal (shaker input) is shown in

Figure 5. Figures 13 to 15 shows the shaker performance with conventional adaptive time domain Filtered-x

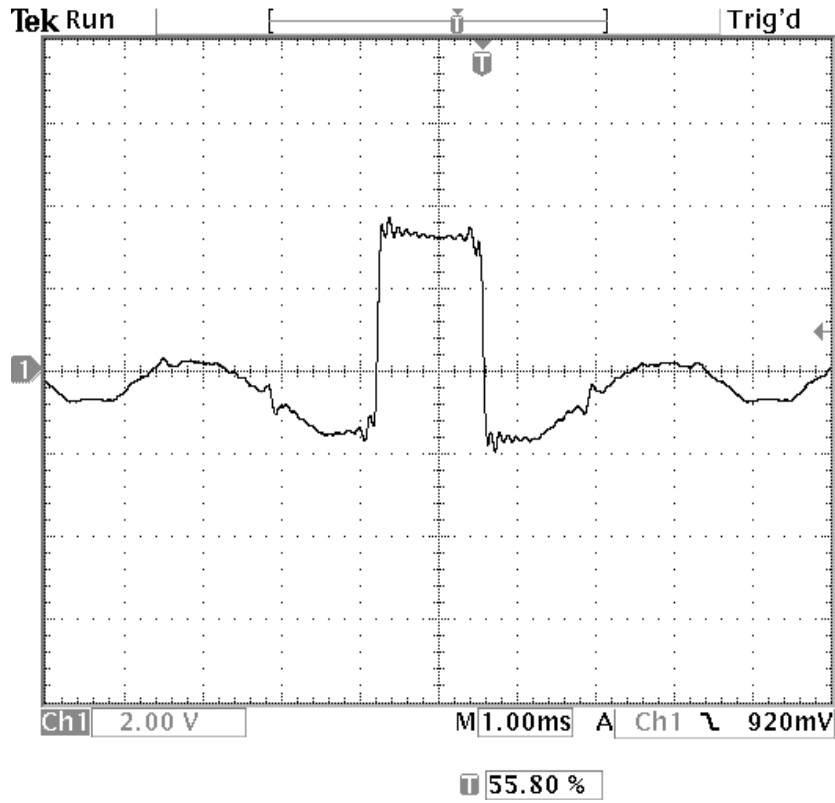


Figure 14. Shaker controlled output (with Filtered-X).

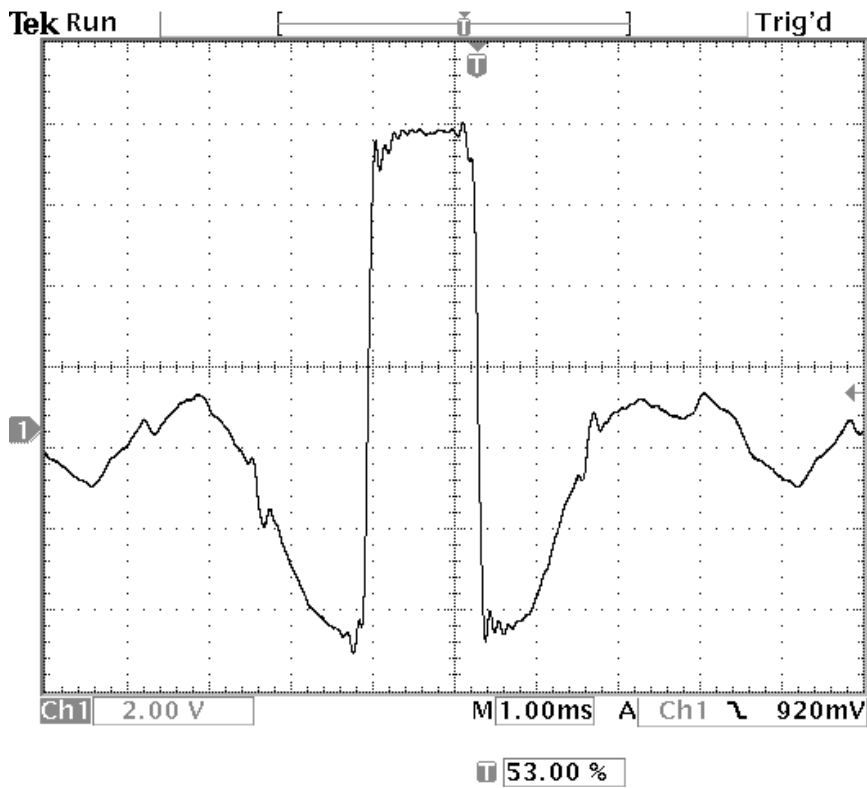


Figure 15. Controller output (shaker input-with Filtered-x).

algorithm used to implement control design for shaker system. During simulation it is found that the PHTFDAF algorithm converges to the desired signal faster than with the conventional frequency domain adaptive filtering (FDAF) method.

REFERENCES

- George FL (1997). *Electrodynamic Shaker Fundamentals*, Sound and Vibration, Data Physics Corporation, San Jose, California. pp. 1-8.
- George FL, Dave S (2001). *Understanding the Physics for Electrodynamic Shaker Performance*, Dynamic reference issue, Sound and Vibration, Data Physics Corporation, San Jose, California. pp. 1-9.
- De Silva CW (2000). *Vibration fundamentals and Practice*, CRC press.
- Frain WE (1977). *Shock wave testing on an Electrodynamic Vibrator*, Applied Physics Laboratory, The Johns Hapkins University Laurel Maryland.
- George FL (1997). *Electrodynamic Shaker Fundamentals*, Sound and Vibration, Data Physics Corporation, San Jose, California.
- George FL, Dave S (2001). *Understanding the Physics for Electrodynamic Shaker Performance*, Dynamic reference issue, Sound and Vibration, Data Physics Corporation, San Jose, California.
- IMV Corporation Japan (2001), *Instruction Manual*.
- Macdonald HM (1994). *Analysis and Control of an Electrodynamic Shaker*, PhD Thesis, Heriot-Watt University, Edinburgh.
- Haykin S (2002). *Adaptive Filter Theory*, Prentice-Hall.
- Olmos S, Sornmo L, Laguna P (2002). *Block Adaptive Filters with Deterministic Reference Inputs for Event-Related Signals: BLMS and BRLS*, IEEE Tran. Sig. Proc., 50(5): 1102-1112.
- Bendel Y, Burshtein D, Shalvi O, Weinstein E (2001). *Delayless Frequency Domain Acoustic Echo Cancellation*, IEEE Trans on Speech and Audio Proc., 9(5): 589-597.
- Valoor MT, Chandrashekhara K, Agarwal S (2000). *Active Vibration control of smart composite plates using self-adaptive neuro-controller*, Smart Mater. Struct., Vol. 9, IOP Publishing Ltd, pp. 197-204.